International Journal of Thermophysics, Vol. 19, No. 2, 1998

Prediction of Fluid Mixture Transport Properties by Molecular Dynamics[1]

D. K. Dysthe,[2] A. H. Fuchs,[2] and B. Rousseau[2, 3]

Equilibrium molecular dynamics simulations of mixtures of *n*-decane with methane, ethane, and carbon dioxide and of the mixture carbon dioxide–ethane were performed using the anisotropic united atoms model for *n*-decane and one- and two-center Lennard–Jones models for the light components. The Green–Kubo relations were used to calculate the viscosity, thermal conductivity, and inter- and intradiffusion. Viscosities are predicted with a maximum deviation of 30% at low gas concentrations and less than 10% deviation at high gas concentrations. The viscosity and thermal conductivity are less sensitive to the cross interactions than the diffusion coefficients, which exhibit deviations between models and with experiments of up to 60%.

KEY WORDS: alkanes; carbon dioxide; diffusion; mixtures; molecular dynamics; thermal conductivity; viscosity.

1. INTRODUCTION

Knowledge of transport properties of multicomponent gases and oils is of great economical importance in reservoir modeling, planning of transport, and design of industrial plants. For mixtures of constituents of dissimilar size, shape, and polarity, traditional prediction methods for viscosity and thermal conductivity need experimental data to fit mixing rules [1], while for diffusion the few existing prediction methods deviate by up to almost an order of magnitude [2]. One possible route to obtaining better predictions is to use molecular dynamics (MD), which can predict thermophysical properties from models of molecular interactions only. Most interaction

[1] Paper presented at the Thirteenth Symposium on Thermophysical Properties, June 22–27, 1997, Boulder, Colorado, U.S.A.

[2] Laboratoire de Chimie Physique des Matériaux Amorphes, Bâtiment 490, Université Paris-Sud, 91405 Orsay Cedex, France.

[3] To whom correspondence should be addressed.

0195-928X/98/0300-0437$15.00/0

models proposed have been applied to transport properties at only one or two state points, and hardly any transport studies have been performed on mixtures. Two recent studies [3, 4] have, however, tried to evaluate four realistic, flexible models of alkanes at one-component fluid states in a more systematic manner. The main criteria for evaluating the models are that they should be (a) *simple*, in order to keep computing time to a minimum; (b) *transferable*, in the sense that the same group parameters can be used for all molecules of the same family; (c) *property independent*, meaning that regressing the parameters for one property should give good predictions of other properties; and (d) *state independent*, i.e., the accuracy of prediction should not depend on the temperature, density, and composition.

In this work, we concentrate on criteria c and d, the property and state independence. More precisely, we use MD and the Green–Kubo (GK) formalism to study transport coefficients as a function of composition at constant temperature and pressure in mixtures of *n*-decane with methane, ethane, and carbon dioxide. These represent mixtures of *n*-decane with a small spherical and two linear, rigid molecules with different quadrupole moments. We have chosen mixtures of dissimilar molecules because the model interaction parameters regressed in the pure fluid, i.e., in a set of like molecules, may not be directly transferable to a group of molecules of different shape, size, and interaction types (for example, polarity).

2. MODELS

As mentioned, we require our models to be simple and transferable and to give predictions that are property and state independent.

For *n*-decane we use the Padilla and Toxvaerd [5] anisotropic united atom (AUA) model, where the CH_i potential centers are displaced from the carbon atom positions. The bonds are modeled by constraining the distance between adjacent CH_i groups. This flexible chain model includes bending and torsional motion as well. This *n*-decane model is the least density and temperature dependent of the currently used flexible UA models [4]. The potential parameters of all the molecular models used in this work are given in Table I. Methane is modeled as a single LJ potential with parameters given by Möller et al. [6]. Ethane and CO_2 are modeled as two-center LJ (2CLJ) models where the distance between the two centers is constrained. Both ethane and CO_2 have considerable quadrupole moments (-1.2 and -4.3 DÅ, respectively), and even though simulated equilibrium properties show reasonable agreement with experiment in a small range of states [7, 8], it is yet unknown to what degree the 2CLJ models satisfy the criteria of property and state independence. The gain in computer time for the 2CLJ model relative to adding a point quadrupole

or partial charges (and a third LJ center for CO_2) is not critical for the model choice; the molecules are small and still quite tractable with current workstations. For pure fluid calculations the models employed in this work are not optimal, even though the results show that the pure fluid transport coefficients are predicted to within the uncertainties. On the other hand, for mixtures of ethane and CO_2 with LJ UA models of alkanes, it is clearly computationally faster (by up to an order of magnitude) to treat cross interactions with LJ mixing rules, $\sigma_{ij} = f(\sigma_{ii}, \sigma_{jj})$ and $\varepsilon_{ij} = g(\varepsilon_{ii}, \varepsilon_{jj})$, rather than adding new interaction potentials for the interactions between the quadrupole or partial charges of ethane and CO_2 with polarizable *n*-alkane sites. For the system ethane–CO_2 there is evidence that one may reproduce "nonideal" effects with the models we have described. Fincham et al. [9] were able to demonstrate azeotropy of this mixture in qualitative agreement with experimental data only by modifying the Lorentz–Berthelot mixing rules: $\varepsilon_{ij} = (1 - k_{ij})\sqrt{\varepsilon_{ii}\varepsilon_{jj}}$, with $k_{ij} = 0.2$ [and $\sigma_{ij} = (\sigma_{ii} + \sigma_{jj})/2$ as normal]. Wang and Cummings [10] reported that, using the parameters of Fincham et al., their NEMD simulations of the viscosity of ethane–CO_2 at a density of 20 mol·l^{-1} and at temperatures ranging from 150 to 280 K reproduced a plateau region as a function of composition. In the CO_2–*n*-decane and CO_2–ethane system we employ both $k_{ij} = 0.2$ and $k_{ij} = 0$ to study the effect on the transport coefficients of the attractive cross interactions. For the ethane–*n*-decane and methane–*n*-decane mixtures we use Lorentz–Berthelot mixing rules.

Table I. Potential Parameters

	σ_{ii} (Å)	ε_{ii}/k_B (K)	m_i (g mol^{-1})	I (Å^2 g mol^{-1})	d_{bond} (Å)
CO_2	3 035	163 3	44	43 124	2 37
C_2H_6	3 52	137 5	30	26 933	2 345
CH_4	3 7327	149 92	16	d_{AUA} (Å)	
CH_3	3 527	120	15	0 275	1 545
CH_2	3 527	80	14	0 37	1 545

Bending potential, $u_\theta = (62{,}543/2)(\cos\theta - \cos 114\,6)^2$ [k_B (K)]

Torsion potential, $u_t = \sum_{i=0} a_i \cos^i\chi$ [k_B (K)]

a_0	a_1	a_2	a_3	a_4	a_5
1037 76	2426 07	81 64	−3129 46	−163 28	−252 73

3. SIMULATION DETAILS

We have employed two MD programs developed independently. The details of the program for workstations [4] (used for methane–*n*-decane and ethane–*n*-decane) and that used on a Cray T3E [11] (used for CO_2–*n*-decane) will be published separately. Both programs use the RATTLE [12] algorithm to solve the constrained equations of motion. In order to study the property independence of the models we have chosen to use the Green–Kubo (GK) formalism, which yields all the transport properties simultaneously; nonequilibrium methods are always property specific. We calculate the viscosity, η, the thermal conductivity, λ, the intradiffusion coefficients, D_a, and the kinetic interdiffusion coefficients, D_{12}^K, by the usual correlation function integrals:

$$\eta = \frac{V}{10k_B T} \int_0^\infty dt \langle \mathbf{P}^{0S}(t) : \mathbf{P}^{0S}(0) \rangle \tag{1}$$

$$\lambda = \frac{V}{3k_B T^2} \int_0^\infty dt \langle \mathbf{J}_q(t) \cdot \mathbf{J}_q(0) \rangle \tag{2}$$

$$D_a = \frac{1}{3N_a} \int_0^\infty dt \sum_{i \in a} \langle \mathbf{v}_i(t) \cdot \mathbf{v}_i(0) \rangle \tag{3}$$

$$D_{12}^K = \frac{V^2}{3Nw_1 w_2 m_1 m_2} \int_0^\infty dt \langle \mathbf{J}_1(t) \cdot \mathbf{J}_1(0) \rangle \tag{4}$$

Here V is the system volume, T the temperature, $\mathbf{P}^{0S}$ the symmetric traceless pressure tensor, $\mathbf{J}_q$ the heat flux, $\mathbf{J}_1$ the mass flux of component 1, $\mathbf{v}_i$ the instantaneous velocity of the center of mass of molecule i, N the total number of molecules, N_a the number of molecules of type a, w_i the mass fraction, m_i the molecular mass, and t the time. We apply the molecular definitions of $\mathbf{P}^{0S}$ and $\mathbf{J}_q$. We have not attempted to correct the thermal conductivity for the lack of partial molar enthalpies in the microscopic heat flux definition [13]. The kinetic interdiffusion coefficient D_{12}^K is connected to the experimentally accessible interdiffusion coefficient $D_{12} = B_x D_{12}^K$ with a thermodynamic factor $B_x = (x_1/RT)(\partial \mu_1/\partial x_1)_{T,P}$, where μ_1 is the chemical potential, x_1 is the mole fraction of component 1, and R is the gas constant.

All the simulations were performed with 108 molecules. Each configuration was equilibrated and stabilized at the desired temperature during 1 ns. The production runs were performed for 4 ns in the NVE ensemble with 4-fs time steps. During each run, 15 subaverages were saved to disk as the basis for statistical analysis. The loss of total energy per nanosecond in an NVE run was never more than 0.3 times the standard deviation of the kinetic energy.

4. RESULTS AND DISCUSSION

We have performed simulations at six or seven compositions of the systems methane–*n*-decane, ethane–*n*-decane, CO_2–ethane, and CO_2–*n*-decane in the mole fraction range $x_1 = 0$ to 1 (let component 1 be the light component or CO_2). For methane–*n*-decane and ethane–*n*-decane, the temperatures were about 333 K and the densities corresponded to 40 MPa. For the CO_2–*n*-decane system we performed two series at temperatures of about 311 and 403 K and densities corresponding to 27.7 and 20 MPa, respectively. The densities were obtained from Reamer and Sage [14] for ethane–*n*-decane, from Reamer et al. [15] for methane–*n*-decane, from Scaife and Lyons [16] for *n*-decane[4] and from Cullick and Mathis [18] for CO_2–*n*-decane. Table II contains the results of all the simulations. The statistical uncertainties are estimated for each single run as the standard deviation of the mean of the 15 subaverages. They are approximately 10% for the viscosity, 10% for the thermal conductivity, $x_i^{-1/2}$% for the intradiffusion coefficients D_i, and $4(x_1x_2)^{-1/2}$% for the kinetic interdiffusion coefficient D_{12}^{K}.

Figures 1 and 4 show that all the viscosity results have much in common. The methane–*n*-decane and pure *n*-decane viscosities displayed in Fig. 1 are compared to experimental data from Knapstad et al. [17], the ethane–*n*-decane viscosities are compared to the empirical correlation of Assael et al. [19], and the CO_2–*n*-decane viscosities are compared to the experimental data of Cullick and Mathis [18]. The simulations underestimate the viscosities by up to 30% for *n*-decane–rich mixtures. At $x_1 > 0.5$ the deviations are not significant. We may distinguish between two causes of the deviations: (a) underestimation of the viscosity of *n*-decane model in the pure fluid at high densities—as the gas content increases, the density decreases and the *n*-decane molecules are less important for the viscosity; and (b) poor modeling of the cross interactions (site–site interactions and the total interaction between different molecules), causing a too large fluidity. Some discrimination of these effects may be obtained from the interesting result that, for CO_2–*n*-decane (Fig. 4), the two curves for $k_{ij} = 0$ and $k_{ij} = 0.2$ hardly differ. At $x_1 = 0.5$ the 13% difference between the two models is not very significant; the error bars overlap. This shows that the viscosity (and thermal conductivity in Table II) is virtually independent of details in the *attractive* site–site cross interaction. The model mixtures employed interpolate the pure component viscosities in a smooth manner, and in the case of CO_2–*n*-decane, the change in the attractive part

[4] The *n*-decane density used was later found to correspond to a pressure of 30 MPa [15, 17] and the results are therefore compared with experiments at the simulated densities or at 30 MPa.

Table II. Simulation Results of the Alkane Mixtures and Alkane–CO_2 Mixtures

k_{ij}	x_1	ρ (kg m ^{3})	T (K)	P (MPa)	$\eta \times 10^3$ (Pa s)	λ (W m^{-1} K^{-1})	$D_{12}^{K} \times 10^9$ (m s^{-1})	$D_1 \times 10^9$ (m s^{-1})	$D_2 \times 10^9$ (m s^{-1})
					CH_4–$C_{10}H_{22}$				
	0 000	728 8	333 6	46 3	0 67	0 15			1 85
	0 093	720 6	328 4	44 0	0 48	0 15	5 9	7 04	1 86
	0 296	691 8	324 9	41 2	0 45	0 13	5 5	7 45	2 22
	0 500	644 1	330 5	45 5	0 23	0 12	7 4	10 4	3 20
	0 704	557 8	334 8	45 0	0 13	0 11	9 0	15 8	4 81
	0 907	375 1	326 8	39 4	0 058	0 083	13 7	30 9	9 42
	1 000	217 6	330 8	38 3	0 027	0 062		55 4	
					C_2H_6–$C_{10}H_{22}$				
	0 120	723 3	331 9	52 6	0 58	0 15	4 7	5 27	1 86
	0 398	683 2	334 6	48 4	0 36	0 14	5 6	7 08	2 54
	0 657	626 4	337 0	52 5	0 24	0 13	6 3	9 54	3 54
	0 870	538 2	330 9	47 6	0 14	0 13	6 6	13 2	5 20
	1 000	419 0	330 2	33 8	0 064	0 10		20 5	
					CO_2–$C_{10}H_{22}$				
	0 000	736 3	312 7	35 8	0 65	0 15			1 48
0 0	0 148	744 9	307 6	30 1	0 63	0 15	5 0		
0 2	0 148	744 9	314 9	42 1	0 63	0 15	5 8		
0 0	0 306	753 4	306 2	21 5	0 46	0 14	4 9		

0.2	0.306	753.4	314.5	42.2	0.46	0.14	5.8			
0.0	0.500	774.1	333.5	50.9	0.35	0.15	5.3			
0.2	0.500	774.1	310.0	44.7	0.40	0.14	5.8			
0.0	0.648	795.5	308.9	25.3	0.25	0.13	4.9			
0.2	0.648	795.5	315.7	54.3	0.25	0.14	7.6			
0.0	0.852	837.7	305.4	16.9	0.17	0.13	4.9			
0.2	0.852	837.7	314.5	47.9	0.17	0.13	6.8			
	1.000	907.4	333.9	44.3	0.11	0.12				
	0.000	682.0	409.5	47.2	0.34	0.13				
0.0	0.148	675.6	405.0	32.0	0.26	0.13	10.4			
0.0	0.306	675.8	406.0	27.7	0.22	0.12	10.8			
0.0	0.500	667.9	407.0	19.1	0.18	0.11	10.4			
0.0	0.852	570.0	409.0	10.9	0.065	0.066	14.0			
	1.000	380.8	395.0	15.4	0.030	0.034				
					CO_2–C_2H_6					
	0.000	598.7	147.5	26.7	0.288	0.220				2.38
0.0	0.250	631.2	210.7	38.6	0.186	0.191	6.01	5.84		5.44
0.2	0.250	631.2	210.3	56.1	0.179	0.178	7.22	5.94		5.60
0.0	0.491	714.6	240.4	24.2	0.136	0.155	7.75	7.88		7.49
0.2	0.491	714.6	240.4	49.1	0.130	0.155	10.0	8.08		7.69
0.0	0.741	799.8	278.1	22.7	0.115	0.133	10.0	10.7		10.0
0.2	0.741	799.8	281.7	45.1	0.113	0.129	13.3	10.8		10.6
	1.000	884.0	277.5	−8.38	0.102	0.106		12.4		

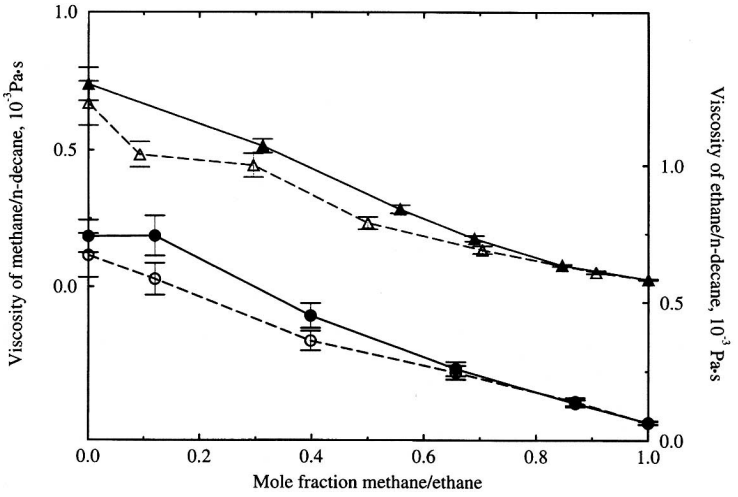

Fig. 1. Viscosity in the methane/*n*-decane and ethane/*n*-decane systems as a function of composition. Open triangles, methane/*n*-decane; open circles, ethane/*n*-decane; open symbols, simulation; filled triangles, experimental; filled circles, experimental (pure fluids) and Assael correlation (mixture).

of the cross interactions does not alter this behavior. This behavior is contrary to what Wang and Cummings [10] observed for CO_2–ethane. We have therefore repeated the simulations of Wang and Cummings and the results (see Table II) show that there is *no* significant[5] difference in the viscosity and thermal conductivity upon changing k_{ij} from 0 to 0.2.

Comparing the two series for CO_2–*n*-decane (see Fig. 4), one observes that when the prediction for pure *n*-decane is better (at low density), the prediction for the region $x_1 \leqslant 0.5$ is better. Comparing all four gas–*n*-decane systems, one observes the tendency that the deviation in the mixture for $x_1 \leqslant 0.5$ is larger than the deviation for pure *n*-decane at the same pressure and temperature. We therefore conclude that the cross-interaction effect of the different molecular shapes and sizes is smaller but may be discriminated from the underestimation caused by the poor *n*-decane potential.

In Figs. 2 and 3, we compare simulation results of the methane–*n*-decane and ethane–*n*-decane systems with diffusion coefficients from Hafskjold and colleagues [2, 20]. The most striking features of the intradiffusion coefficients are the overestimation of D_1 at low gas concentrations ($x_1 < 0.6$) and the underestimation of D_2 at low *n*-decane concentrations

[5] The standard deviation for this system is 8%.

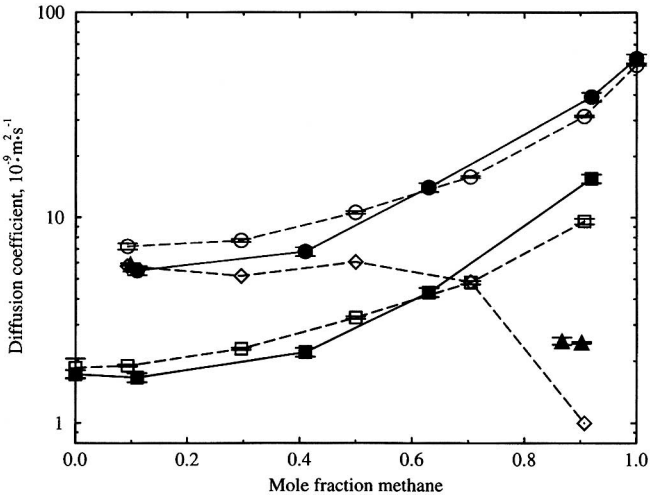

Fig. 2. Diffusion in the methane/*n*-decane system as a function of composition. Open circles, D_{methane} from MD; filled circles, D_{methane} from experiment; open squares, D_{decane} from MD; filled squares, D_{decane} from experiment; open diamonds, $D_{12} = B_x D_{12}^{\text{K}}$ from MD; filled triangles, experimental D_{12}.

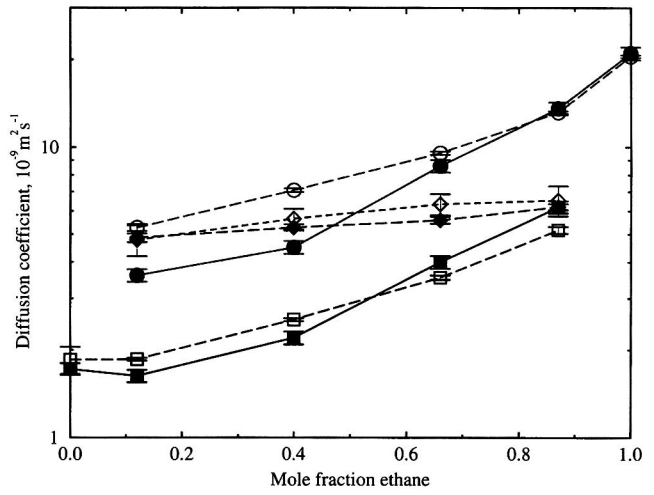

Fig. 3. Diffusion in the ethane/*n*-decane system as a function of composition. Open circles, D_{ethane} from MD; filled circles, D_{ethane} from experiment; open squares, D_{decane} from MD; filled squares, D_{decane} from experiment; filled diamonds, $D_{12}^{\text{K}} = x_1 D_2 + x_2 D_1$ from MD; open diamonds, D_{12}^{K} from MD.

($x_1 > 0.6$). In the methane–*n*-decane system the deviation reaches 35% for both methane and *n*-decane at $x_1 = 0.093$ and $x_1 = 0.907$, respectively. Ethane diffusion is overestimated by as much as 57% at $x_1 = 0.398$, and *n*-decane is underestimated by 17% at $x_1 = 0.87$. The large deviations in D_i at low concentrations of type i in the mixture is a clear sign that the *cross* interactions are not well represented. The interdiffusion coefficient in the CO_2–*n*-decane and CO_2–ethane systems is very much affected by the change in k_{ij} (see Fig. 4 and Table II). The reduction in attractive cross interaction makes D_{12}^{K} increase over the whole composition range, with a maximum increase of 55%. The diffusion results of the CO_2–ethane system show that the interdiffusion coefficient is much more sensitive to the attractive site–site interaction than the intradiffusion coefficient. In sum, the diffusion coefficients are, in contrast to the viscosity and thermal conductivity, sensitive to both the steric effects of shape and size and the imprecision of the pure *n*-decane potential and the interdiffusion coefficient is very sensitive to the attractive site–site cross interaction.

For methane–*n*-decane we have included three experimental points for D_{12}. In order to compare with the simulations we have calculated B_x

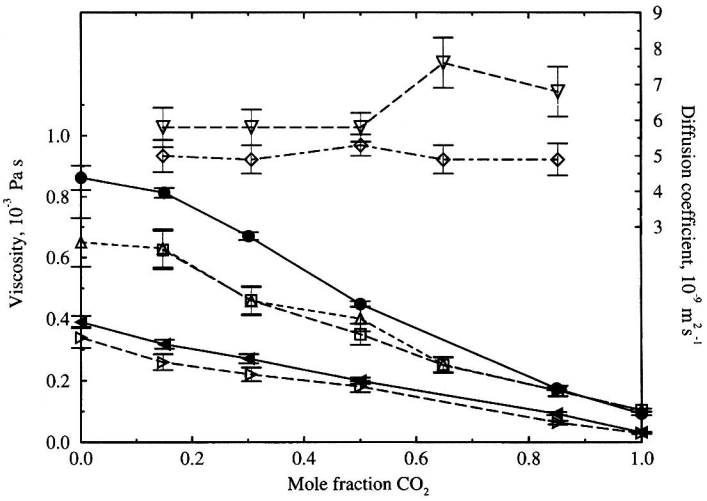

Fig. 4. Viscosity and interdiffusion in the CO_2/*n*-decane system as a function of composition. Open squares, simulated (sim.) viscosity at 311 K with $k_{ij} = 0.0$; upward open triangles, sim. viscosity at 311 K with $k_{ij} = 0.2$; filled circles, experimental viscosity at 311 K; open diamonds, sim. interdiffusion at 311 K with $k_{ij} = 0.0$; downward open triangles, sim. interdiffusion at 311 K with $k_{ij} = 0.2$; rightward open triangles, sim. viscosity at 403 K with $k_{ij} = 0.0$; leftward filled triangles, experimental viscosity at 411 K.

using the Peng–Robinson equation of state, setting the binary interaction parameter to 0.0265. At $x_1 = 0.093$, where $B_x = 0.98$, the difference between simulation and experiment is only 4%. At $x_1 = 0.907$ the D_{12} deduced from simulation is 60% too low. Because of the incorrect analytical form of the equation of state on approaching the critical point, one must expect B_x and thus D_{12} from simulation to be no more than qualitatively correct for $x_1 > 0.5$. In Fig. 3 we have also included a comparison of the Darken approximation to $D^{K}_{12,D} = x_1 D_2 + x_2 D_1$ with D_1 and D_2 from simulation. There is no significant deviation between D^{K}_{12} and $D^{K}_{12,D}$ for either methane–*n*-decane, ethane–*n*-decane, or CO_2–ethane with $k_{ij} = 0$, but the deviation is 20% for CO_2–ethane with $k_{ij} = 0.2$.

Our final comment is that if one compares the simulated thermal conductivities of ethane–*n*-decane and methane–*n*-decane with the Assael correlation, one finds that the differences are never greater than the uncertainty.

5. CONCLUSIONS

We have performed MD simulations of three mixtures of dissimilar molecules over the whole range of compositions, using simple one- and two-center LJ models for the light components methane, ethane, and CO_2 and the flexible AUA model for *n*-decane. The viscosities are always underpredicted, with a maximum deviation of 30% at a low gas content and a mean deviation of 16%. The diffusion coefficients are both under- and overestimated by up to 60%. The study has, to a certain degree, separated three principal causes of the deviations: (a) the imprecision of the pure *n*-decane potential (all transport coefficients are affected), (b) the steric size and shape effects (the diffusion coefficients are more strongly affected than the viscosity and thermal conductivity), and (c) the effects of the attractive cross interactions (the viscosity and thermal conductivity are not significantly affected, the intradiffusion coefficients are weakly affected, and the interdiffusion is strongly affected). In sum, the potential models utilized seem both composition and property dependent, but the causes (and remedies) need to be investigated further.

ACKNOWLEDGMENTS

We thank Marc Durandeau for initiating this work and for fruitful discussions. We would like to thank Total Exploration Production for a grant to one of us (D.K.D). We thank the Institut du Dévelopement et des Ressources en Informatique Scientifique (IDRIS) for the generous allocation of Cray T3E computer time.

REFERENCES

1. W. D. Monnery, W. Y. Svrcek, and A. K. Mehrotra, *Can. J. Chem. Eng.* **73**:3 (1995).
2. M. Helbaek, B. Hafskjold, D. K. Dysthe, and G. H. Sørland, *J. Chem. Eng. Data* **41**:598 (1996).
3. W. Allen and R. L. Rowley, *J. Chem. Phys.* **106**:10273 (1997).
4. D. K. Dysthe, A. H. Fuchs, and B. Rousseau, in preparation.
5. P. Padilla and S. Toxvaerd, *J. Chem. Phys.* **94**:5653 (1991).
6. D. Möller, J. Oprzynski, A. Müller, and J. Fisher, *Mol. Phys.* **75**:363 (1992).
7. K. Singer, A. Taylor, and J. V. L. Singer, *Mol. Phys.* **33**:1757 (1977).
8. M. Wojcik, K. E. Gubbins, and J. G. Powles, *Mol. Phys.* **45**:1209 (1982).
9. D. Fincham, N. Quirke, and D. J. Tildesley, *J. Chem. Phys.* **84**:4535 (1986).
10. B. Y. Wang and P. T. Cummings, *Mol. Simulat.* **10**:1 (1993).
11. B. Rousseau and J.-M. Simon, in preparation.
12. H. C. Andersen, *J. Comput. Phys.* **52**:24 (1983).
13. J.-M. Simon, D. K. Dysthe, A. H. Fuchs, and B. Rousseau, *Fluid Phase Equil.*, in press.
14. H. H. Reamer and B. H. Sage, *J. Chem. Eng. Data* **7**:161 (1962).
15. H. H. Reamer, R. H. Olds, B. H. Sage, and W. N. Lacey, *Ind. Eng. Chem.* **34**:1526 (1942).
16. W. G. Scaife and C. G. Lyons, *Ber. Bunsenges. Phys. Chem.* **94**:758 (1990).
17. B. Knapstad, P. A. Skjolsvik, and H. A. Øye, *Ber. Bunsenges. Phys. Chem.* **94**:1156 (1990).
18. A. S. Cullick and M. L. Mathis, *J. Chem. Eng. Data* **29**:393 (1984).
19. M. J. Assael, J. H. Dymond, M. Papadaki, and M. P. Patterson, *Int. J. Thermophys.* **13**:659 (1992).
20. D. K. Dysthe, B. Hafskjold, J. Breer, and D. Čejka, *J. Phys. Chem.* **99**:11230 (1995).